VanNieuwenhove I, Salomon A, Peters K, Graulus G, Martins JC, Frankel D, Kersemans K, DeVos F, VanVlierberghe S, Dubruel P. Gelatin- and starch-based hydrogels. Part A: Hydrogel development, characterization and coating. *Carbohydrate Polymers* 2016

DOI: http://dx.doi.org/10.1016/j.carbpol.2016.06.098

Gelatin- and starch-based hydrogels. Part A: Hydrogel development, characterization and coating.

Ine Van Nieuwenhove[1], Achim Salamon[2], Kirsten Peters[2], Geert-Jan Graulus[1], José C. Martins[3], Daniel Frankel[4], Ken Kersemans[5], Filip De Vos[5], Sandra Van Vlierberghe[1, 6]*, Peter Dubruel[1]*

* Corresponding authors: sandra.vanvlierberghe@ugent.be , peter.dubruel@ugent.be

1) Polymer Chemistry & Biomaterials Group - Ghent University, Krijgslaan 281, Building S4-Bis, BE-9000 Ghent

2) Department of Cell Biology - Rostock University Medical Center, Schillingallee 69, D-18057 Rostock

3) NMR and Structure Analysis Research Group - Ghent University Krijgslaan 281, Building S4, BE-9000 Ghent

4) School of Chemical Engineering and Advanced Materials - University of Newcastle, Mertz Court, Claremont Road, UK-NE1 7RU Newcastle Upon Tyne

5) Laboratory of Radiopharmacy - Ghent University Ottergemsesteenweg 460, BE-9000 Ghent

6) Brussels Photonics Team – Vrije Universiteit Brussel Pleinlaan 2, BE-1050 Brussels

Abstract

The present work aims at constructing the ideal scaffold matrix of which the physico-chemical properties can be altered according to the targeted tissue regeneration application. Ideally, this scaffold should resemble the natural extracellular matrix (ECM) as close as possible both in terms of chemical composition and mechanical properties. Therefore, hydrogel films were developed consisting of methacrylamide-modified gelatin and starch-pentenoate building blocks because the ECM can be considered as a crosslinked hydrogel network consisting of both polysaccharides and structural, signaling and cell-adhesive proteins. For the gelatin hydrogels, three different substitution degrees were evaluated including 31%, 72% and 95%. A substitution degree of 32% was applied for the starch-pentenoate building block. Pure gelatin hydrogels films as well as interpenetrating networks with gelatin and starch were developed. Subsequently, these films were characterized using gel fraction and swelling experiments, high resolution-magic angle spinning ^{1}H NMR spectroscopy, rheology, infrared mapping and atomic force microscopy. The results indicate that both the mechanical properties and the swelling extent of the developed hydrogel films can be controlled by varying the chemical composition and the degree of substitution of the methacrylamide-modified gelatin applied. The storage moduli of the developed materials ranged between 14 and 63 kPa. Phase separation was observed for the IPNs for which separated starch domains could be distinguished located in the surrounding gelatin matrix. Furthermore, we evaluated the affinity of aggrecan for gelatin by atomic force microscopy and radiolabeling experiments. We found that aggrecan can be applied as a bioactive coating for gelatin hydrogels by a straightforward physisorption procedure. Thus, we achieved distinct fine-tuning of the physico-chemical properties of these hydrogels which render them promising candidates for tissue engineering approaches.

Key words: gelatin, starch, biomaterials, aggrecan, tissue engineering

Formatted: Font: (Default) Times New Roman, 12 pt

1. Introduction

The lack of acutely available organs for transplantation is a worldwide issue which is even expected to worsen as the world population ages. Tissue engineering is an approach aiming at bridging this gap.(Furth, Atala, & Van Dyke, 2007; Griffith & Naughton, 2002; Langer R, 1993; Langer, 1997; Lemons, 2013) In this approach, cells are seeded onto scaffolds or implants to develop into functional tissues.(Drury & Mooney, 2003; Gomillion & Burg, 2006; C. Liu, Xia, & Czernuszka, 2007; Lutolf & Hubbell, 2005; Peters et al., 2009) In addition, an increasing number of procedures can be found in literature which rely on the application of stem cells.(Barry & Murphy, 2004; Gomillion & Burg, 2006; Griffith & Naughton, 2002; Jeffrey M. Gimble et al., 2007; Peters et al., 2009) Using mesenchymal stem cells (MSC), the present study aims at a scaffold guided strategy towards tissue regeneration. The constructed scaffold is a three-dimensional matrix serving as a surrogate extracellular matrix (ECM) enabling cell attachment and promoting cell proliferation as well as differentiation. The design of a scaffold resembling the natural ECM is preferred in order to mimic as closely as possible the natural aqueous environment that cells are experiencing.(Chen, Wang, Wei, Mo, & Cui, 2010; Kim, Kim, & Salih, 2005; Kuo, Chen, Hsiao, & Chen, 2015) This natural ECM can be considered as a crosslinked hydrogel network consisting of polysaccharides as well as structural, signaling and cell-adhesive proteins. Taking this knowledge into consideration, it is of great interest to evaluate the potential of polymer networks mimicking this ECM composition. Therefore, gelatin and starch are applied as natural building blocks in the present work, representing both the protein and polysaccharide constituent of the natural ECM.

Gelatin is derived from collagen, which is the most abundant structural protein in mammals.(Di Lullo, Sweeney, Korkko, Ala-Kokko, & San Antonio, 2002) In addition, it is generally non-immunogenic and retains informational signals including an arginine-glycine-aspartic acid (RGD) sequence which promotes cell adhesion, differentiation and proliferation.(Gautam, Dinda, & Mishra, 2013) These properties and its unique gel-forming ability render gelatin an interesting biopolymer towards tissue engineering applications.(Awad, Quinn Wickham, Leddy, Gimble, & Guilak, 2004; Dubruel et al., 2007; Li et al., 2005; Nichol et al., 2010) Starch, on the other hand, consists of a mixture of the polysaccharides amylose and amylopectin. The relative ratio of amylose to amylopectin strongly depends on the starch source considered. The application of starch offers several advantages including its biodegradability and ease of processing.(Azevedo, Gama, & Reis, 2003; Puppi, Chiellini, Piras, & Chiellini, 2010) Starch-based polymers as well as blends have already been introduced as promising biomaterials for bone and cartilage tissue engineering applications due to these advantages. For instance, Mendes et al. (2001) showed the potential of starch/ethylene vinyl alcohol blends reinforced with hydroxyapatite for temporary bone replacement implants.(Mendes et al., 2001) Raafat et al. (2013) developed a hydrogel series composed of starch/N-vinylpyrrolidone which were proven to exhibit *in vitro* bioactivity and blood compatiblity.(Raafat, Eldin, Salama, & Ali, 2013) Moreover, gelatin and starch are often

combined for several food processing applications.(Burey, Bhandari, Rutgers, Halley, & Torley, 2009; Firoozmand, Murray, & Dickinson, 2009; MARRS, 1982)

In this work, hydrogels were developed consisting of either a gelatin phase or the combination of both a starch and a gelatin phase. In the latter case, these hydrogels are so-called interpenetrating polymer networks (IPNs) if the appropriate crosslinking strategy is applied ensuring both building blocks to be covalently crosslinked but not bonded to each other.(V et al., 2007) The potential of gelatin hydrogels in contact with adipose tissue derived mesenchymal stem cells (adMSCs) was already demonstrated by Peters et al. (2009) towards the adhesion of these cells.(Peters et al., 2009) Therefore, we selected the gelatin hydrogels as reference material for the IPNs of starch and gelatin. Pure starch hydrogels were not applied as these hydrogels were shown to be too brittle to process them in hydrogel films. To the best of our knowledge, we first reported on the combination of starch and gelatin in IPNs for the purpose of tissue engineering applications. Indeed, previous results reported by Van Nieuwenhove et al. (2015) on starch-based hydrogels were promising since the hydrogels developed in contact with adMSC were shown to be biocompatible.(Van Nieuwenhove et al., 2015)

IPNs have gained an increased attention the last decades mainly due to their high potential as hydrogels for biomedical applications.(Dragan, 2014) However, most of the hybrid IPNs hydrogels, reported in literature, are obtained by either combining various polysaccharides or synthetic polymers and proteins with synthetic polymers.(Dragan, 2014; La Gatta, Schiraldi, Esposito, D'Agostino, & De Rosa, 2009; Peng, Yu, Mi, & Shyu, 2006; Pescosolido et al., 2011) Only a few papers report on the combination of proteins and polysaccharides for the construction of (semi)-IPNs.(Cui, Jia, Guo, Liu, & Zhu, 2014; Y. Liu & Chan-Park, 2009; Picard, Doumèche, Panouillé, & Larreta-Garde, 2010; Turgeon & Beaulieu, 2001)

The present work focusses on the construction of the ideal scaffold matrix of which the physico-chemical properties can be altered according to the targeted tissue regeneration application. The latter is highly relevant as natural tissue is also characterized by different mechanical properties. Thus, altering the mechanical properties of the constructed hydrogel films is of great interest. For instance breast tissue, mainly composed of adipose tissue, is characterized by a storage modulus of 3.2 kPa(Abbas, Judit, & Donald, 2007), whereas the storage modulus of articular cartilage is in the range of 2 to 7 GPa(Silver, Bradica, & Tria, 2002). Due to their soft and rubbery consistence, hydrogels do not reveal such high storage moduli. However, these hydrogels can still be applicable as coating onto implants to target orthopedic applications.

For this reason, hydrogel films were prepared with varying chemical composition (i.e. ratio between gelatin and starch phase) and varying degree of substitution (DS) of the gelatin phase applied. First, gelatin and starch were chemically modified with photo-crosslinkable moieties. This modification enables their subsequent processing into hydrogel films and ensures sufficient stability of the materials upon *in vitro* application. In addition, the present work will evaluate whether a bioactive coating of aggrecan, the main articular cartilage constituent, can be deposited

onto the materials via physisorption. More specifically, liquid atomic force microscopy and radiolabeling experiments will be performed to study this hydrogel coating.

2. Experimental section

2.1. Materials

For all the synthesis experiments, gelatin (type B), from bovine bone origine, was applied (Rousselot, Gent, Belgium). Furthermore, dimethyl sulfoxide (DMSO, 99.85%) was purchased from Acros (Geel, Belgium) and purified via distillation before use. Irgacure® 2959 was applied as photo-initiator (BASF, Kaisten, Switzerland) and dithiothreitol (Fisher Scientific, Erembodegem, Belgium) was used as a bifunctional thiol-based crosslinker agent. All other chemicals were purchased from Sigma Aldrich (Bornem, Belgium) and were used as received unless stated otherwise. The radiolabeling experiments were performed using Iodogen (1,3,4,6-tetrachloro-3a,6a-diphenyl-glycouril) obtained from Pierce (USA) and using a radioiodide solution (125I: Perkin Elmer, Massachusetts, USA).

2.2. Synthesis of hydrogel building blocks

Both the pentenoate-modified starch (SP) and the methacrylamide-modified gelatin (gel-MA) were synthesized as described earlier.(Peters et al., 2009; Van Nieuwenhove et al., 2015) In brief, corn starch was dissolved in DMSO (5 w/v%, 70 °C), a catalytic amount of dimethylaminopyridine was added and the reaction mixture was stirred for 20 minutes. Subsequently, 4-pentenoic anhydride (37.5 equivalents with respect to the saccharide units) was added and reacted overnight. The purified product was obtained via precipitation in ethanol, followed by dialysis against double distilled water (MWCO: 12,000 – 14,000 Da) and freeze-drying by means of a Christ freeze-dryer alpha 2-4-LSC.

For the gelatin derivatives, the amount of crosslinkable side chains was adjusted by varying the amount of methacrylic anhydride added. Three different modifications were performed using 0.5, 1 and 2.5 equivalents methacrylic anhydride added with respect to the primary amines present along the gelatin backbone.

2.3.Hydrogel production

Hydrogel films were prepared through covalent crosslinking. For this purpose, a gel-MA solution (10 w/v%) was crosslinked via photo-induced polymerization in the presence of 2 mol% Irgacure® 2959 upon applying UV-A irradiation for 30 minutes (with an intensity of 10 mW/cm² and a wavelength range of 250-450 nm). IPNs were obtained by the addition of one equivalent of DTT and Irgacure® 2959 to various SP (5 w/v%) and gel-MA solutions (10 w/v%) which were

subsequently exposed to UV-A irradiation. The addition of DTT is needed as the crosslinking of SP occurred via a radical thiol-ene reaction.

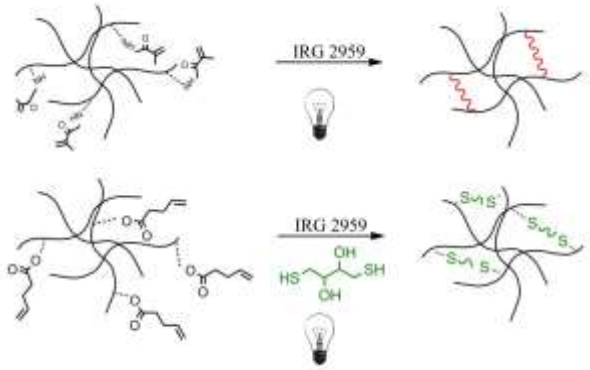

Figure 1 UV-Crosslinking of methacrylamide-modified gelatin solution (top) upon the addition of Irgacure 2959® and starch-pentenoate (below) upon the addition of Irgacure 2959® and a bifunctional thiolcrosslinker.

2.4. Characterization of the hydrogels developed

2.4.1. Gel fraction and swelling experiments

Samples (ϕ = 1.4 mm, thickness = 1 mm) of the crosslinked hydrogels were incubated in double-distilled water at 37°C in order to determine the gel fraction of the crosslinked hydrogels. As a result, polymer chains that were not covalently linked into the network were able to leach out from the hydrogels by diffusion. The gel fraction can be calculated, expressed as the percentage of material which is chemically incorporated in the three-dimensional network (equation 1).

$$gel\ fraction\ (\%) = \frac{W_d}{W_{d0}} . 100 \quad (1)$$

with W_d = dry weight after swelling
W_{d0}= dry weight before swelling

All the measurements were performed in duplicate. The results are presented as mean values with corresponding standard deviations (SD).

For the swelling experiments, the hydrogel films were submerged in double-destilled water at 37°C, and the changes in mass were recorded as a function of time. At distinct time points, the

samples were removed from the medium, dipped on a piece of paper in order to remove adhered solution to the surface, and weighed. Afterwards, the samples were again incubated in the swelling medium.

The swelling percentage can be defined as:

$$Swelling\ (\%) = \frac{W_{ht} - W_{d0}}{W_{d0}} .100 \quad (2)$$

with W_{do} = weight of dry gel at initial time 0

W_{ht} = weight of hydrated gel at time t

All these experiments were performed in duplicate. The results are reported as mean values with corresponding SD.

2.4.2. Determination of crosslinking efficiency via HR-MAS ^{1}H-NMR spectroscopy

High Resolution Magic Angle Spinning ^{1}H NMR spectroscopy (HR-MAS) was performed in order to evaluate the crosslinking efficiency (CE) of the developed hydrogel films. A Bruker Avance II 700 spectrometer (700.13 MHz) device was used applying a HR-MAS probe equipped with a ^{1}H, ^{13}C, ^{119}Sn and gradient channel. The spinning rate was adjusted to 6 kHz.

On the day of the experiments, a small amount of the freeze-dried hydrogels was placed inside a 4 mm zirconium oxide MAS rotor (50 µl) and a few microliters of deuterium oxide (D_2O) were added enabling the samples to swell. A teflon-coated cap was applied in order to close the rotor. Prior to analysis the HR-MAS samples were homogenized by manual stirring. Afterwards, the spectra were analyzed after baseline correction.

The CE is calculated using the following equation (Sandra Van Vlierberghe José C. Martins, and Peter Dubruel, 2010):

$$CE\ (\%) = \left[\frac{\left(\frac{I^{i}_{5.75\ or\ 5.1\ ppm}}{I^{i}_{1.1\ ppm}}\right) - \left(\frac{I^{c}_{5.75\ or\ 5.1\ ppm}}{I^{c}_{1.1\ ppm}}\right)}{\left(\frac{I^{i}_{5.75\ or\ 5.1\ ppm}}{I^{i}_{1.1\ ppm}}\right)}\right] x\ 100 \quad (3)$$

This equation (3) is based on the comparison of the intensity of the signals characterizing the protons of the introduced double bonds, before and after crosslinking. Normalization is applied by using the inert signal at 1.1 ppm, because different samples need to be compared.

2.4.3. Rheology

The mechanical properties of the hydrogels were investigated via oscillation rheology with a rheometer type Physica MCR-301 (Anton Paar, Sint-Martens-Latem, Belgium) running with Physica Rheoplus software. All measurements were performed using a plate-plate geometry. More specifically, a hydrogel sample was placed between two parallel plates (diameter upper plate = 25 mm), after which the upper plate was adjusted to ensure close contact of each sample with both plates. Tests were performed using oscillatory sine functions and upon applying a frequency of 1 Hz and a gap setting of 0.95 mm. In addition, a 0.05% strain was selected to perform the oscillatory measurements as the linear visco-elastic range ranges from 0 to about 0.3% strain (data not shown). In the present work, the different hydrogels were measured under these settings while monitoring the storage (G') and the loss moduli (G").

2.4.4. Atomic Force Microscopy and IR-mapping

Atomic force microscopy (AFM) experiments were performed with a Nanoscope IIIa Multimode (Digital Instruments, Santa Barbara, California, USA) applying 'tapping mode' in air. Measurements were performed on spincoated gelatin/starch solutions (10 w/v % gelatin and 5 w/v% starch solution) since AFM measurements require flat surfaces. In addition, spincoated gelatin and starch solutions were also measured separately as references. The nanoscope software version 4.43r8 was used to process all data obtained with AFM. On the other hand, IR-mapping was performed on dried hydrogel films using a Perkin Elmer Spectrum 100 FT-IR spectrometer with a Spotlight 400 FT-IR imaging system. Therefore, the hydrogel surfaces were scanned using IR mapping to evaluate the absorbance potentially occurring at the characteristic wavenumbers for gelatin and starch in order to determine the presence of both building blocks in the hydrogel samples."

Formatted: Font: (Default) Times New Roman, 12 pt

Formatted: Font: (Default) Times New Roman, 12 pt

2.5. Characterization of bioactive coating

In the present work, AFM and radiolabeling experiments were utilized in order to determine the interaction between gelatin and aggrecan.

2.5.1. AFM under liquid conditions

AFM experiments were conducted on an Agilent 5500 AFM/SPM microscope in a liquid environment at 20 °C.

2.5.1.1. Topographic AFM imaging

Prior to AFM imaging, aggrecan from bovine plasma was dissolved in phosphate buffered saline (PBS) to acquire a stock solution of 1 mg/ml. The aggrecan solution was diluted to the desired

concentration and added onto the gelatin hydrogel film for 30 minutes at room temperature followed by three PBS washing steps prior to imaging. The washing steps were essential to remove loosely bound aggrecan.

Images were obtained in tapping mode using silicon tips (Nanosensors, series PPP-NCSTR-50) with a resonance frequency within a range from 76 to 263 kHz and a force constant of 12 – 29 N/m. Typical scan rates were in the range of 0.5 – 1 kHz at a resolution of 512 points/line. All measurements were performed in PBS.

2.5.1.2. Force spectroscopy

Force spectroscopy measurements were performed using a backside aluminium coated silicon cantilever (Cont GB-G, Budget Sensor) with a nominal spring constant of 0.02 N/m and a resonant frequency of 13 kHz. Accurate measurement of spring constants was obtained using the equipartition theorem (Thermal K)(Hutter & Bechhoefer, 1993). Forces of interaction between the aggrecan and the hydrogel were measured by functionalizing the AFM tip with aggrecan through a physisorption process by incubation of the tip for 30 minutes. Prior to monitoring the aggrecan interactions with the gel, force distance curves were acquired on bare mica in order to confirm that the tip was successfully functionalized. Force spectroscopy experiments were performed on the gelatin samples at four locations defined by the user. Approximately 1000 – 1500 force-distance curves were obtained per location.

For the analysis of the data obtained, Scanning Probe Image Processor (SPIP) version 6.2.8 (Image Metrology, Lyngby, Denmark) was used. Interaction forces between the aggrecan and the gel were derived from the registered force distance curves. Histograms of the height features as well as the rupture forces were created with Sigmaplot (Systat Software, San Jose, CA). For the rupture force distributions of aggrecan, the selected curves were fitted to a Gaussian function in order to extract the average rupture force.

2.5.2. Radiolabeling experiments

Radioiodination was performed by a slightly modified method described by Pierce Biotechnology Inc. (Rockford, IL, USA; www.piercenet.com). In brief: Iodogen was dissolved in chloroform to a concentration of 2 mg/mL and 100 µL was added to a 5 mL conical vial. The solvent was then evaporated under a gentle N_2 flow at room temperature and the Iodogen-coated vials were stored in a dessicator at 5 °C prior to use. A stock solution of aggrecan (0.5 mg/ml, 1.5 ml) was added to a Iodogen coated reaction vessel, immediately followed by the addition of 20 µL radioiodide solution (^{125}I). This mixture was incubated for 20 minutes at room temperature under slight shaking. Free iodine was removed by G-25 Sephadex gel filtration (GE Healthcare, Belgium), equilibrated with 0.01 M phosphate buffer of pH 7. The overall radiochemical purity (RCP) was then determined using iTLC-SG chromatographic strips (Gel- man Sciences) and a citrate-buffer

(0.068 M citrate, pH 7.4) as eluent. From this ^{125}I-aggrecan solution dilutions were prepared to adjust the concentration of aggrecan to 0.5, 0.3, 0.2, 0.1 and 0.05 mg/mL. The procedure for coating the hydrogel films is similar to the aforementioned in section 1.5.1.1.

3. Results and discussion

3.1 In-depth physico-chemical characterization of the hydrogels

Gelatin and starch were modified with UV-crosslinkable side-groups enabling their subsequent processing into hydrogel films. Gelatin was successfully modified with varying amount of methacrylic anhydride.(Peters et al., 2009; Salamon et al., 2014) In this way, the influence of the DS on the mechanical properties could be evaluated. The modification was confirmed and quantified via ^{1}H-NMR spectroscopy for the different gelatin derivatives (see figure S1). The methacrylamide-modified gelatins (gel-MA) in the present work possess a DS of 31, 72 and 95% with respect to the primary amines available along the gelatin backbone. In addition to the functionalized gelatin, starch was successfully modified using 4-pentenoic anhydride yielding starch-pentenoate (SP) with a DS of 32%.(Van Nieuwenhove et al., 2015) This DS was also quantified by means of ^{1}H-NMR spectroscopy and is expressed as the amount of modified repeating saccharide units (see figure S1).

Subsequently, hydrogel films of both gel-MA and gel-MA in combination with SP were prepared via film casting followed by chemical crosslinking. This enabled the characterization of the developed materials via several techniques. Pure starch hydrogels were not developed as these hydrogels were not robust enough to enable manipulation.

3.1.1. Gel fraction and swelling experiments

First, the gel fractions and the equilibrium swelling degree of the developed materials were determined. The results are listed in table 1 and to facilitate further discussion each hydrogel sample is designated with a unique code. On the one hand, gel-MA x% indicates hydrogels purely based on gelatin which are characterized by their DS represented by x%. On the other hand, the abbreviation SP1 reflects the presence of a SP content of 10% and SP2 assigns the IPNs defined by 20% SP content. The gel fraction results indicate an efficient crosslinking during which most of the crosslinkable moieties were consumed resulting in gel fractions of 85% and higher. In general, thus, well-established networks were formed as almost no leaching occurred of unbound molecules. As anticipated, it can be observed in table 1 that the gel fraction will increase with an increasing DS for gelatin hydrogels. This because a higher DS will result in a more crosslinked hydrogel network going from gel-MA 31% to 95%.

A small decrease in the gel fraction can be observed for the hydrogel samples with a starch content of 20% compared to 10% and the hydrogels without starch. However, conversely, an

increase in total amount of crosslinkable moieties is noticeable with an increasing amount of starch present in the polymer network (see last column table 1). It can be hypothesized that upon the introduction of a critical amount of starch (i.e. 20%), the phase separation between starch and gelatin will be more pronounced causing the starch to be more clustered together in domains. The occurrence of phase separation will still be tackled in depth in section 2.1.4.

Therefore, it is hypothesized that upon introducing this critical amount of starch the gel fraction again decreases because the starch domains leach out during incubation (cfr. these domains can be considered as starch-only hydrogels, which do not enable manipulation as already indicated above). This effect is not demonstrated in the hydrogel samples with a 10% starch content, since the starch hydrogel building blocks will be more randomly distributed in a gelatin phase.

The swelling experiments show that all hydrogel types are able to absorb large quantities of water. Indeed, equilibrium swelling degrees ranging from 660% up to 4100% were observed for the hydrogel samples developed. These results are in good agreement with the results obtained by Graulus et al. (2015) for gelatin hydrogels and hydrogels consisting of gelatin and alginate.(Graulus et al., 2015)

Table 1 Gel fractions (%) for the various hydrogel samples and the number of crosslinkable moieties present in the precursor solutions (methacrylamide for gel-MA versus pentenoate for the starch phase). All measurements were performed in duplicate and the results are presented as mean values with corresponding standard deviations (SD) (n=2).

Code	Composition (v%)		Gel fraction (%) ± SD	mol MA moieties / ml precursor solution	mol pentenoate moieties / ml precursor solution	mol total amount of crosslinkable moieties/ ml precursor solution
	gel-MA	SP				
gel-MA 31%	100	-	85 ± 5	1.19E-05	-	1.19E-05
gel-MA 72%	100	-	94 ± 1	2.77E-05	-	2.77E-05
gel-MA 72% - SP1	90	10	100 ± 1	2.49E-05	9.87E-06	3.48E-05
gel-MA 72% - SP2	80	20	86 ± 4	2.22E-05	1.97E-05	4.19E-05
gel-MA 95%	100	-	98 ± 1	3.66E-05	-	3.66E-05
gel-MA 95% - SP1	90	10	100 ± 9	3.29E-05	9.87E-06	4.28E-05
gel-MA 95% - SP2	80	20	93 ± 7	2.93E-05	1.97E-05	4.90E-05

3.1.2. Evaluation of crosslinking efficiency

The crosslink efficiency (CE) of the UV-cured hydrogels was evaluated by means of HR-MAS ^{1}H-NMR spectroscopy. This technique evaluates the consumption of double bonds upon crosslinking and is thus a measure for the efficiency of crosslinking.(Sandra Van Vlierberghe José C. Martins, and Peter Dubruel, 2010) Conventional ^{1}H-NMR spectroscopy does not enable the characterization of crosslinked polymer networks due to the considerable line broadening which results from the presence of dipolar couplings and magnetic susceptibility effects.(Ramadhar, Amador, Ditty, & Power, 2008; Shapiro, Chin, Marti, & Jarosinski, 1997) HR-MAS spectroscopy circumvents this line broadening by rapidly rotating the sample at a magic angle of 54.7° with respect to the static magnetic field, following swelling of the material.(Ramadhar et al., 2008) This swelling induces sufficient, solution-like, rotational mobility of the polymer.(Sandra Van Vlierberghe José C. Martins, and Peter Dubruel, 2010) Highly crosslinked hydrogel materials will thus exhibit a reduced chain mobility and will show broader peaks compared to less crosslinked materials.(Rueda, Suica, Komber, & Voit, 2003)

The CE could only be calculated for the gelatin phase based on equation (3). Unfortunately, the CE of the starch phase could not be calculated separately due to overlap of the characteristic peaks of the starch and gelatin phase both present in the IPNs. Therefore, equation (3) is only applicable for the gelatin phase present in the IPNs. It is important to emphasize that the CE reflects a ratio between the amount of double bounds consumed upon crosslinking to the amount initially present in the samples.

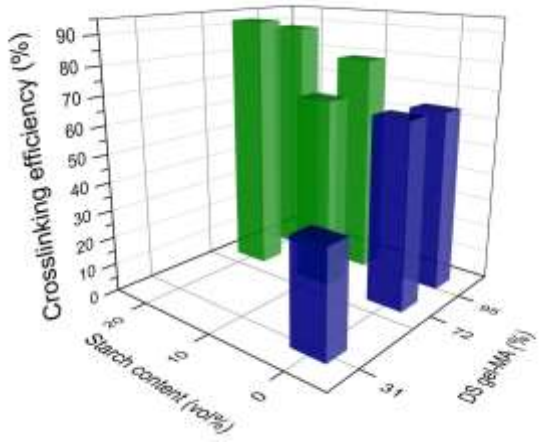

Figure 2 3D-plot representing the gelatin crosslinking efficiency (CE, z-axis) (%) of the various hydrogel films as a function of the starch content (x-axis) and the degree of substitution of methacrylamide-modified gelatin (gel-MA) hydrogels (axis).

The CE values of the applied gelatin phase for the various hydrogel films are represented in figure 2. In addition to these results, table 2 represents the calculated amount of network points present in the gelatin phase taking into account the amount of photocrosslinkable MA side groups present in the network and the CE.

The results for the pure gelatin hydrogels are in good correlation with previous reported results for hydrogels crosslinked under similar conditions.(Salamon et al., 2014) However, the latter paper did not comprise a comparison of different DS of gel-MA. Figure 2 indicates an increasing CE with increasing DS for the hydrogels solely consisting of a gelatin phase (blue bars). This increase is observed until a maximum in CE is reached at a DS of 72%, since the crosslinking efficiencies for gel-MA 72% and 95% are in the same range. The trend of increasing CE with increasing DS can be anticipated as more crosslinkable side groups will be incorporated along the backbone for a higher DS (see table 2). Thus, more double bonds will be in closer proximity, and, therefore more likely to react upon photo-crosslinking. Moreover, the CE remains similar between the pure gelatin film compared to the IPNs with a 10% starch content (SP1 hydrogel samples in table 2). An increase in CE is observed, however, upon addition of a 20% starch phase. The latter phenomenon is anticipated to be the result of a more pronounced phase separation occurring between starch and gelatin present in the IPNs which is more likely to occur for the SP2 gelatin-starch IPNs as already highlighted in the previous section. This phase separation ensures the gelatin chains to exist in closer proximity despite the presence of an additional starch phase within the polymer network.

Table 2 Comparison of the amount of networks points in the gelatin phase with the amount of crosslinkable moieties in this gelatin phase for the various gelatin hydrogels samples developed as well as the interpenetrating networks based on gelatin and starch.

Code	mol MA moieties/ ml precursor solution	CE (%)	mol MA network points/ ml precursor solution
gel-MA 31%	1.19E-05	37	4.39E-06
gel-MA 72%	2.77E-05	65	1.82E-05
gel-MA 72% - SP1	2.49E-05	67	1.68E-05
gel-MA 72% - SP2	2.22E-05	92	2.04E-05
gel-MA 95%	3.66E-05	64	2.35E-05
gel-MA 95% - SP1	3.29E-05	79	2.59E-05
gel-MA 95% - SP2	2.93E-05	88	2.58E-05

3.1.3. m ination of mechanical properties

Rheology was applied to examine the mechanical properties of the developed hydrogels. Polymer materials typically exhibit visco-elastic behavior which implies that a recovery occurs at a certain delay after deformation. As anticipated, an improvement in mechanical properties is observed for more densely crosslinked hydrogels.(Hutson et al., 2011; Nichol et al., 2010; Van Den Bulcke et al., 2000; Wang et al., 2014) This trend can be derived from figure 3 for the gel-MA and gel-MA SP1 series along the y-axis: the storage modulus (G') increases with increasing DS of gel-MA.

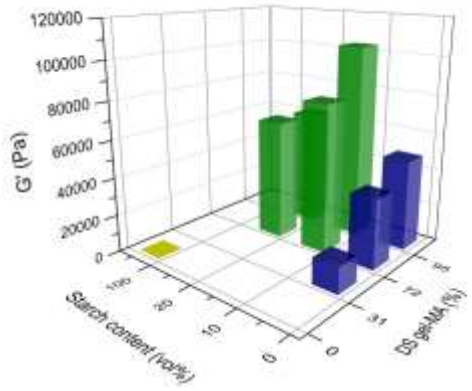

Figure 3 3D plot representing the storage modulus G' of the various hydrogels (z-axis) as a function of the starch content (%) (x-axis) and the degree of substitution of methacrylamide-modified gelatin (gel-MA) (y-axis).

Although HR-MAS ^{1}H NMR spectroscopy indicated the highest CE for gel-MA 72%, there is a lower absolute number of network points present compared to gel-MA 95% (see last column table 2). Therefore, the hydrogel films consisting of gel-MA 95% are characterized by a higher G'-value as these networks are more crosslinked. Moreover, G' shifts to higher values for the IPNs with a starch-content of 10%. The mechanical properties are thus improved upon introducing an additional starch phase in the gelatin network. For the IPNs with 10% starch content (SP1), the trend along the y-axis remains similar: G' increases with increasing DS of gel-MA. A more crosslinked gelatin phase thus results in improved mechanical properties. Conversely, the IPNs with 20% starch content (SP2) again exhibit lower G' values than the IPNs with 10% starch (SP1). It can be anticipated that the addition of a critical amount of starch will result in a more pronounced phase separation, as already indicated above. In addition, the gel fraction results complement the data and trends as derived from rheology.

3.1.4. Topographical characterization

The gelatin-starch IPNs were further investigated by AFM and IR mapping in order to study relevant phase separation phenomena.(Dazzi et al., 2012; Ferrer, Sánchez, Ribelles, Colomer, &

Pradas, 2007) First of all, AFM is applied, a technique being part of the family of scanning probe microscopes which scan across a surface monitoring probe-sample interactions. The measurements were performed on spincoated gelatin/starch-solutions, since AFM experiments require flat surfaces. In addition, spincoated gelatin and starch-solutions were also measured separately as reference.

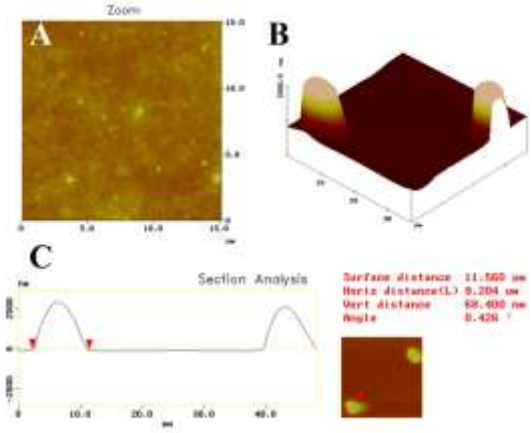

Figure 4 A. Top view of methacrylamide-modified gelatin (gel-MA) B. 3D surface plot of 90% gel-MA + 10% starch-pentenoate C. Section analysis of starch granules present in a gelatin matrix.

The mixtures of gelatin and starch explicitly show smaller regions of phase-separated starch granules being present adjacent to the globular domains of gelatin. These granules are separate domains possessing a size of approximately 10 µm (figure 4).

In addition to AFM, the incorporation of starch in the gelatin matrix was also evaluated by means of IR mapping of the characteristic wavenumbers of either gelatin (eg. 1633 cm^{-1}) or starch (eg. 1017 and 1079 cm^{-1}). The results of the air-dried gel-MA 72%-SP1 hydrogel are depicted in figure 5, together with the ATR-IR spectra of the starting materials. The results obtained from IR mapping clearly confirm the phase separation occurring between gelatin and starch. A separate starch domain was observed in the gelatin matrix exhibiting absorbance at the characteristic wavenumbers corresponding with C-O bond stretching. Moreover, the size of this starch domain is around 10 µm, which is in correlation with the AFM data (figure 4). Phase separation between mixtures of gelatin and starch was already reported earlier.(Firoozmand et al., 2009; Firoozmand, Murray, & Dickinson, 2012; Khomutov, Lashek, Ptitchkina, & Morris, 1995; Whitehouse, Ashby, Abeysekera, & Robards, 1996) This phenomenon is mainly depending on the thermal conditions, the carbohydrate molecular structure and the properties of the aqueous solution including temperature, pH and ionic strength.(Firoozmand et al., 2012) Firoozmand et al. (2009) also observed phase separation between gelatin and starch in high-sugar gelled systems

consisting of a constant gelatin content (7 wt%) and variable oxidized starch content (from 0 up to 6 wt%).(Firoozmand et al., 2009) For this specific type of system, a microstructure could be observed exhibiting both gelatin- and starch-rich regions with these regions ranging in size from a few micrometers up to twenty micrometers observed via optical microscopy. However, it is important to emphasize that the phase separation and the size of the domains was highly dependent on the specific thermal treatment of the samples.

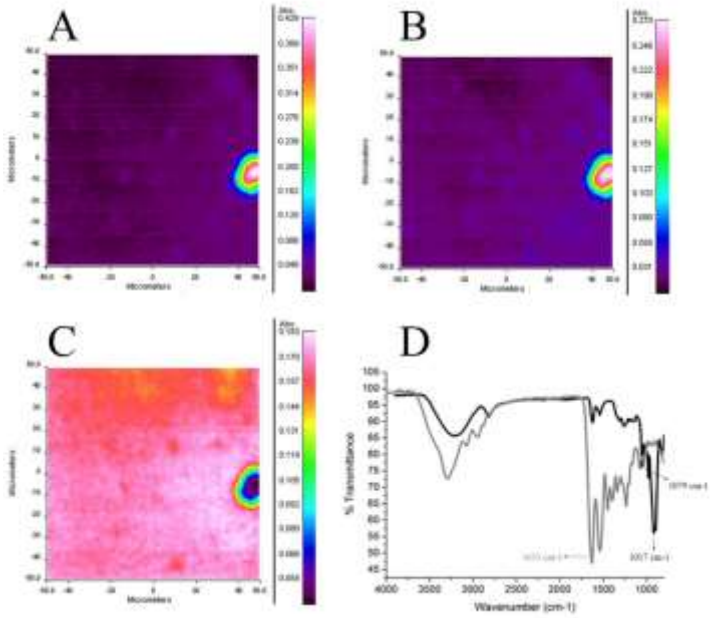

Figure 5 IR spectroscopy data of a dry gel-MA 72%-SP1 starch hydrogel film, including an IR map depicting the absorbance at A. 1017 cm^{-1} , B. 1079 cm^{-1}, C. 1633 cm^{-1} and D. the ATR-IR spectra of gel-MA (light grey) and starch-pentenoate (dark grey).

3.2. Bioactive coating of gelatin hydrogels: aggrecan under investigation

The application of cell-interactive ECM-based coatings is crucial when it comes to tissue engineering, as these coatings can positively influence the cell growth(Altankov et al., 2000; Franck et al., 2013; Heller et al., 2015; Shin, Jo, & Mikos, 2003). In the present paper, aggrecan was selected as a component of the ECM to be applied on the gelatin hydrogels. To the best of our knowledge, no data is yet reported on the application of an aggrecan coating onto gelatin. Aggrecan is a major structural proteoglycan of the cartilage extracellular matrix with a molecular mass higher than 2500 kDa.(Kiani, Chen, Wu, Yee, & Yang, 2002) This molecule consists of numerous chondroitin and dermatan sulphate chains

attached to a core protein. In the present work, AFM and radiolabeling studies were performed in order to determine the interaction between gelatin and aggrecan.

First, AFM was selected to examine the interaction between aggrecan and gelatin, as it allows real-time imaging under liquid conditions, while providing a means to interrogate forces of interaction at picoNewton resolution. The coated gelatin hydrogels were visualized by means of tapping mode AFM before and after coating of the hydrogel surface with the proteoglycan (see figure 6). At a concentration of 50 µg/ml of aggrecan, no distinct features appear in the topographic image of the coated hydrogel. Moreover, the height features detected are within the same range as a non-coated gelatin hydrogel sample (see figures 6A and 6B). Thus, for this concentration, no aggrecan can be detected on top of the gelatin hydrogels. The results from figure 6C clearly show that features between 1.5 and 3 nm and even up to 6 nm are present on the gelatin surface after aggrecan coating at a minimal concentration of 200 µg/ml. For a concentration of 500 µg/ml, a high number of features sized between 1.5 and 2.5 nm can be detected which indicates the presence of more aggrecan on the surface of the gelatin hydrogel.

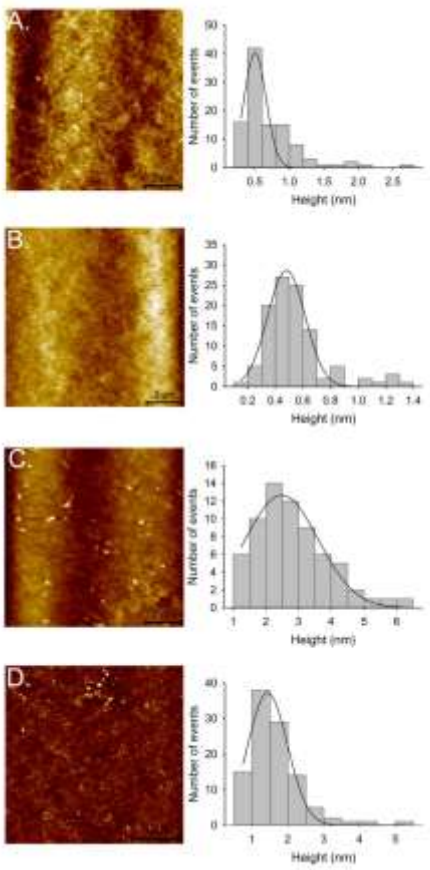

Figure 6 Topographic atomic force microscopy images of spincoated, crosslinked methacrylamide-modified gelatin sample A. without aggrecan-coating and at an aggrecan concentration of B. 50 µg/ml, C. 200 µg/ml, and D. 500 µg/ml. Images were obtained in liquid environment (PBS) at 20°C applying tapping mode.

Following topographic imaging of the surface, force spectroscopy experiments were performed to further characterize the gelatin-aggrecan affinity. For this reason, the operation mode was switched to contact mode and the AFM tip was functionalized with aggrecan. This procedure of tip functionalization via physical interactions allows dangling aggrecan molecules to be "pulled off" the surface that they are in contact with.(Florin et al., 1995) Figure 7 represents the force-distance curves obtained for the gel-MA samples and thus reflecting the adhesion force between aggrecan and gelatin. These forces of interaction between aggrecan and the hydrogel slightly increase from 0.97 to 1.25 nN with increasing DS of gel-MA. The forces detected are in the same range compared to the forces detected between proteins and biomaterial surfaces including

collagen and hyaluronic acid.(Donlon, Nordin, & Frankel, 2012; Herman-Bausier & Dufrene, 2016)

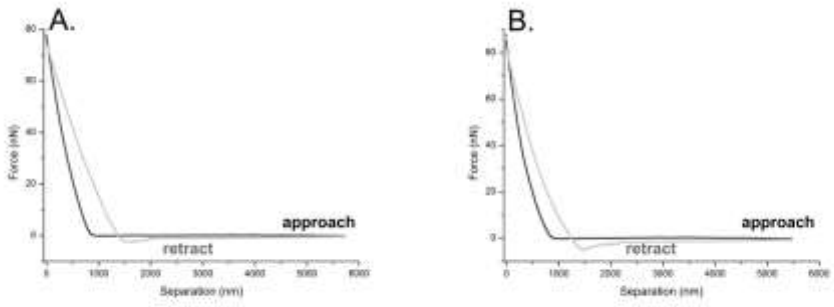

Figure 7 Force spectroscopy experiments of functionalized aggrecan-AFM tip absorbed on spincoated methacrylamide-modified gelatin samples with a degree of substitution of A. 71 % , and B. 94 %

In a second part of the affinity study, radiolabeling experiments were performed enabling the determination of the absolute mass of bound aggrecan. For these experiments, aggrecan was radiolabeled with ^{125}I, and subsequently, a series of different concentrations of radiolabeled aggrecan was coated on top of the gelatin hydrogels. The experiments were performed in triplicate and the mean values and corresponding standard deviations are depicted in figure 8. The results clearly indicate a dose-responsive signal which is nearly linear within the studied concentration range from 50 to 500 µg/ml aggrecan. It can be concluded that the radiolabeling experiments enable characterization of the aggrecan/gelatin affinity at lower concentrations (i.e. 50 µg/ml) than liquid AFM which could only visualize concentrations starting from 200 µg/ml aggrecan.

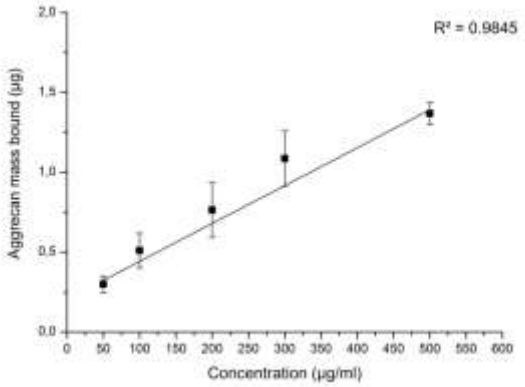

Figure 8 Adsorbed aggrecan amount (µg) as a function of the aggrecan concentration (µg/ml) applied on methacrylamide-modified gelatin measured by radiolabeling experiments.

4. Conclusions

With the aim to investigate how the physico-chemical properties of biopolymer-based hydrogel films can be fine-tuned, hydrogel films were developed with varying chemical composition and degree of substitution of the functionalized gelatin. It can be concluded that the mechanical properties of the hydrogels can be fine-tuned depending on the degree of substitution of the methacrylamide-modified gelatin as well as the chemical composition (i.e. ratio gelatin/starch). The latter is reflected by the storage modulus of the developed materials which ranges from 14 to 63 kPa. Furthermore, phase separation was observed for the IPNs as separated starch domains were present in the gelatin matrix. In addition, the present work also aimed at studying the affinity of aggrecan for gelatin. This affinity was successfully demonstrated via liquid atomic force microscopy and radiolabelling experiments. Thus, it can be concluded that gelatin-based hydrogels can be coated with aggrecan via physisorption. In a forthcoming paper, an *in vitro* cell assay will be performed using human mesenchymal stem cells in order to evaluate the adipogenic as well as osteogenic differentiation potential of the hydrogels developed herein

~~In the subsequent 'part B' of this paper, all hydrogels developed will be evaluated for their potential to support adipose as well as osteogenic tissue regeneration in an *in vitro* approach based on human mesenchymal stem cells. In addition, the effectivity of a bioactive coating on top of the gelatin hydrogels films on these differentiation pathways will be assessed.~~

Formatted: Font: (Default) Times New Roman, 12 pt

Acknowledgment

I. Van Nieuwenhove would like to thank Ghent University for the financial support with a doctoral fellowship 'BOF-mandaat' and the Research Foundation-Flanders (FWO, Belgium) for a travel grant (K213414N). S. Van Vlierberghe would like to acknowledge the FWO for

595 financial support under the form of a research grant (‘Development of the ideal tissue engineering
596 scaffold by merging state-of-the-art processing techniques’, FWO Krediet aan Navorsers) as well
597 as Ghent University for the granted associate professorship. P. Dubruel would like to
598 acknowledge the Alexander von Humboldt Foundation for the financial support under the form
599 of a granted Research Fellowship. The 700 MHz used in this work was funded through the
600 FFEU-ZWAP initiative of the Flemish Government and the Hercules foundation (grant number
601 AUGE-09-006). All authors acknowledge the funding obtained for the EuroTransBio (ETB)
602 Project ETB-2012-33 ‘‘Autologous Stem Cell-Enriched Scaffolds for Soft Tissue
603 Regeneration—ASCaffolds’’.
604

Supporting information

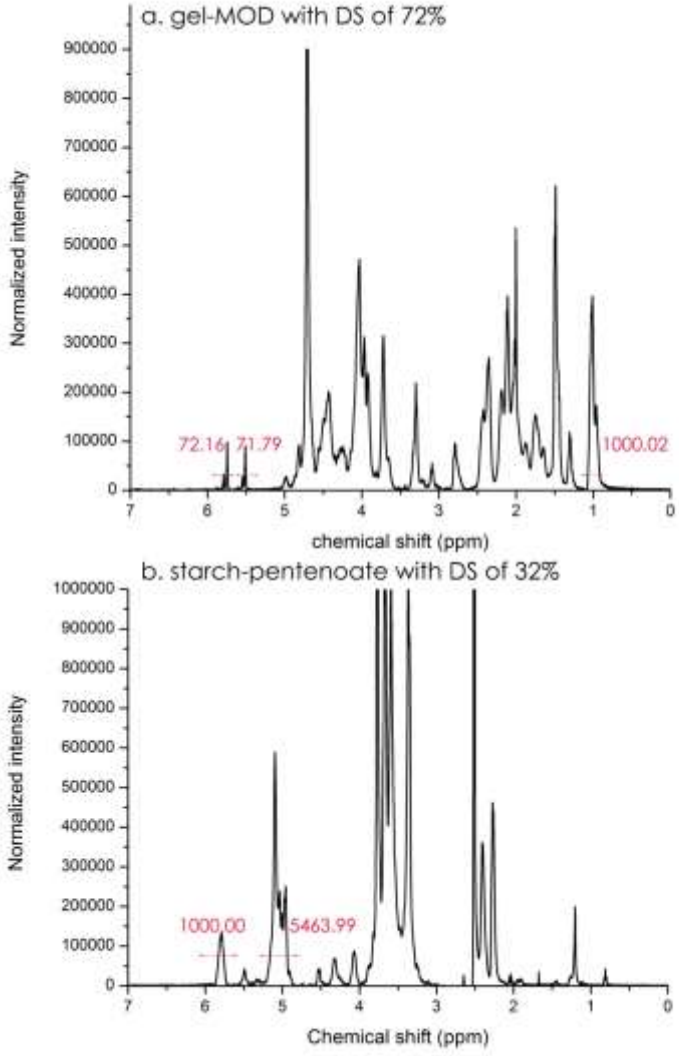

Figure S 1 ^{1}H NMR spectrum of a. gel-MA in D_2O at 40°C , b. starch-pentenoate in DMSO-d6 at 60°C.

609 Abbas, S., Judit, Z., & Donald, P. (2007). Elastic moduli of normal and pathological human breast tissues:
610 an inversion-technique-based investigation of 169 samples. *Physics in Medicine and Biology*, *52*(6),
611 1565. Retrieved from http://stacks.iop.org/0031-9155/52/i=6/a=002

612 Altankov, G., Thom, V., Groth, T., Jankova, K., Jonsson, G., & Ulbricht, M. (2000). Modulating the
613 biocompatibility of polymer surfaces with poly(ethylene glycol): Effect of fibronectin. *Journal of*
614 *Biomedical Materials Research*, *52*(1), 219–230. http://doi.org/10.1002/1097-
615 4636(200010)52:1<219::aid-jbm28>3.0.co;2-f

616 Awad, H. A., Quinn Wickham, M., Leddy, H. A., Gimble, J. M., & Guilak, F. (2004). Chondrogenic
617 differentiation of adipose-derived adult stem cells in agarose, alginate, and gelatin scaffolds.
618 *Biomaterials*, *25*(16), 3211–3222. http://doi.org/http://dx.doi.org/10.1016/j.biomaterials.2003.10.045

619 Azevedo, H. S., Gama, F. M., & Reis, R. L. (2003). In Vitro Assessment of the Enzymatic Degradation of
620 Several Starch Based Biomaterials. *Biomacromolecules*, *4*(6), 1703–1712.
621 http://doi.org/10.1021/bm0300397

622 Barry, F. P., & Murphy, J. M. (2004). Mesenchymal stem cells: clinical applications and biological
623 characterization. *The International Journal of Biochemistry & Cell Biology*, *36*(4), 568–584.
624 http://doi.org/http://dx.doi.org/10.1016/j.biocel.2003.11.001

625 Burey, P., Bhandari, B. R., Rutgers, R. P. G., Halley, P. J., & Torley, P. J. (2009). Confectionery Gels: A
626 Review on Formulation, Rheological and Structural Aspects. *International Journal of Food*
627 *Properties*, *12*(1), 176–210. http://doi.org/10.1080/10942910802223404

628 Chen, Z. G., Wang, P. W., Wei, B., Mo, X. M., & Cui, F. Z. (2010). Electrospun collagen–chitosan
629 nanofiber: A biomimetic extracellular matrix for endothelial cell and smooth muscle cell. *Acta*
630 *Biomaterialia*, *6*(2), 372–382. http://doi.org/http://dx.doi.org/10.1016/j.actbio.2009.07.024

631 Cui, L., Jia, J., Guo, Y., Liu, Y., & Zhu, P. (2014). Preparation and characterization of IPN hydrogels
632 composed of chitosan and gelatin cross-linked by genipin. *Carbohydrate Polymers*, *99*, 31–38.
633 http://doi.org/http://dx.doi.org/10.1016/j.carbpol.2013.08.048

634 Dazzi, A., Prater, C. B., Hu, Q., Chase, D. B., Rabolt, J. F., & Marcott, C. (2012). AFM‐IR:
635 Combining Atomic Force Microscopy and Infrared Spectroscopy for Nanoscale Chemical
636 Characterization. *Applied Spectroscopy*, *66*(12), 1365–1384. http://doi.org/10.1366/12-06804

637 Di Lullo, G. A., Sweeney, S. M., Korkko, J., Ala-Kokko, L., & San Antonio, J. D. (2002). Mapping the
638 ligand-binding sites and disease-associated mutations on the most abundant protein in the human,
639 type I collagen. *The Journal of Biological Chemistry*, *277*(6), 4223–4231.
640 http://doi.org/10.1074/jbc.m110709200

641 Donlon, L., Nordin, D., & Frankel, D. (2012). Complete unfolding of fibronectin reveals surface
642 interactions. *Soft Matter*, *8*(38), 9933–9940. http://doi.org/10.1039/C2SM26315G

643 Dragan, E. S. (2014). Design and applications of interpenetrating polymer network hydrogels. A review.
644 *Chemical Engineering Journal*, *243*, 572–590.
645 http://doi.org/http://dx.doi.org/10.1016/j.cej.2014.01.065

646 Drury, J. L., & Mooney, D. J. (2003). Hydrogels for tissue engineering: scaffold design variables and
647 applications. *Biomaterials*, *24*(24), 4337–4351. http://doi.org/http://dx.doi.org/10.1016/S0142-
648 9612(03)00340-5

649 Dubruel, P., Unger, R., Van Vlierberghe, S., Cnudde, V., Jacobs, P. J. S., Schacht, E., & Kirkpatrick, C. J.

650 (2007). Porous Gelatin Hydrogels: 2. In Vitro Cell Interaction Study. *Biomacromolecules*, *8*(2),
651 338–344. http://doi.org/10.1021/bm0606869

652 Ferrer, G. G., Sánchez, M. S., Ribelles, J. L. G., Colomer, F. J. R., & Pradas, M. M. (2007). Nanodomains
653 in a hydrophilic–hydrophobic IPN based on poly(2-hydroxyethyl acrylate) and poly(ethyl acrylate).
654 *European Polymer Journal*, *43*(8), 3136–3145.
655 http://doi.org/http://dx.doi.org/10.1016/j.eurpolymj.2007.05.019

656 Firoozmand, H., Murray, B. S., & Dickinson, E. (2009). Microstructure and rheology of phase-separated
657 gels of gelatin + oxidized starch. *Food Hydrocolloids*, *23*(4), 1081–1088.
658 http://doi.org/http://dx.doi.org/10.1016/j.foodhyd.2008.07.013

659 Firoozmand, H., Murray, B. S., & Dickinson, E. (2012). Microstructure and elastic modulus of mixed gels
660 of gelatin + oxidized starch: Effect of pH. *Food Hydrocolloids*, *26*(1), 286–292.
661 http://doi.org/http://dx.doi.org/10.1016/j.foodhyd.2011.06.007

662 Florin, E. L., Rief, M., Lehmann, H., Ludwig, M., Dornmair, C., Moy, V. T., & Gaub, H. E. (1995).
663 Sensing specific molecular interactions with the atomic force microscope. *Biosensors and*
664 *Bioelectronics*, *10*(9–10), 895–901. http://doi.org/http://dx.doi.org/10.1016/0956-5663(95)99227-C

665 Franck, D., Gil, E. S., Adam, R. M., Kaplan, D. L., Chung, Y. G., Estrada, C. R., & Mauney, J. R. (2013).
666 Evaluation of Silk Biomaterials in Combination with Extracellular Matrix Coatings for Bladder
667 Tissue Engineering with Primary and Pluripotent Cells. *PLoS ONE*, *8*(2), e56237.
668 http://doi.org/10.1371/journal.pone.0056237

669 Furth, M. E., Atala, A., & Van Dyke, M. E. (2007). Smart biomaterials design for tissue engineering and
670 regenerative medicine. *Biomaterials*, *28*(34), 5068–5073.
671 http://doi.org/http://dx.doi.org/10.1016/j.biomaterials.2007.07.042

672 Gautam, S., Dinda, A. K., & Mishra, N. C. (2013). Fabrication and characterization of PCL/gelatin
673 composite nanofibrous scaffold for tissue engineering applications by electrospinning method.
674 *Materials Science and Engineering: C*, *33*(3), 1228–1235.
675 http://doi.org/http://dx.doi.org/10.1016/j.msec.2012.12.015

676 Gomillion, C. T., & Burg, K. J. L. (2006). Stem cells and adipose tissue engineering. *Biomaterials*,
677 *27*(36), 6052–6063. http://doi.org/http://dx.doi.org/10.1016/j.biomaterials.2006.07.033

678 Graulus, G.-J., Mignon, A., Van Vlierberghe, S., Declercq, H., Feher, K., Cornelissen, M., … Dubruel, P.
679 (2015). Cross-linkable alginate-graft-gelatin copolymers for tissue engineering applications.
680 *EUROPEAN POLYMER JOURNAL*, *72*, 494–506. http://doi.org/10.1016/j.eurpolymj.2015.06.033

681 Griffith, L. G., & Naughton, G. (2002). Tissue engineering--current challenges and expanding
682 opportunities. *Science*, *295*(5557), 1009–1014. Retrieved from
683 http://search.proquest.com/docview/213597341?accountid=11077

684 Heller, M., Kämmerer, P. W., Al-Nawas, B., Luszpinski, M.-A., Förch, R., & Brieger, J. (2015). The
685 effect of extracellular matrix proteins on the cellular response of HUVECS and HOBS after covalent
686 immobilization onto titanium. *Journal of Biomedical Materials Research Part A*, *103*(6), 2035–
687 2044. http://doi.org/10.1002/jbm.a.35340

688 Herman-Bausier, P., & Dufrene, Y. F. (2016). Atomic force microscopy reveals a dual collagen-binding
689 activity for the staphylococcal surface protein SdrF. *MOLECULAR MICROBIOLOGY*, *99*(3), 611–
690 621. http://doi.org/10.1111/mmi.13254

691 Hutson, C. B., Nichol, J. W., Aubin, H., Bae, H., Yamanlar, S., Al-Haque, S., … Khademhosseini, A.
692 (2011). Synthesis and Characterization of Tunable Poly(Ethylene Glycol): Gelatin Methacrylate
693 Composite Hydrogels. *Tissue Engineering Part A*, *17*(13-14), 1713–1723.
694 http://doi.org/10.1089/ten.tea.2010.0666

695 Hutter, J. L., & Bechhoefer, J. (1993). CALIBRATION OF ATOMIC-FORCE MICROSCOPE TIPS
696 (VOL 64, PG 1868, 1993). *Review of Scientific Instruments*, *64*(11), 3342.
697 http://doi.org/10.1063/1.1144449

698 Jeffrey M. Gimble, Adam J. Katz, Bunnell, B. A., Gimble, J. M., Katz, A. J., & Bunnell, B. A. (2007).
699 Adipose-derived stem cells for regenerative medicine. *Circulation Research*, *100*(9), 1249–1260.
700 http://doi.org/10.1161/01.res.0000265074.83288.09

701 Khomutov, L. I., Lashek, N. A., Ptitchkina, N. M., & Morris, E. R. (1995). Temperature-composition
702 phase diagram and gel properties of the gelatin-starch-water system. *CARBOHYDRATE*
703 *POLYMERS*, *28*(4), 341–345. http://doi.org/10.1016/0144-8617(96)00001-X

704 Kiani, C., Chen, L., Wu, Y. J., Yee, A. J., & Yang, B. B. (2002). Structure and function of aggrecan. *Cell*
705 *Res*, *12*(1), 19–32. Retrieved from http://dx.doi.org/10.1038/sj.cr.7290106

706 Kim, H.-W., Kim, H.-E., & Salih, V. (2005). Stimulation of osteoblast responses to biomimetic
707 nanocomposites of gelatin–hydroxyapatite for tissue engineering scaffolds. *Biomaterials*, *26*(25),
708 5221–5230. http://doi.org/http://dx.doi.org/10.1016/j.biomaterials.2005.01.047

709 Kuo, C.-Y., Chen, C.-H., Hsiao, C.-Y., & Chen, J.-P. (2015). Incorporation of chitosan in biomimetic
710 gelatin/chondroitin-6-sulfate/hyaluronan cryogel for cartilage tissue engineering. *Carbohydrate*
711 *Polymers*, *117*(0), 722–730. http://doi.org/http://dx.doi.org/10.1016/j.carbpol.2014.10.056

712 La Gatta, A., Schiraldi, C., Esposito, A., D'Agostino, A., & De Rosa, A. (2009). Novel poly(HEMA-co-
713 METAC)/alginate semi-interpenetrating hydrogels for biomedical applications: Synthesis and
714 characterization. *Journal of Biomedical Materials Research Part A*, *90A*(1), 292–302.
715 http://doi.org/10.1002/jbm.a.32094

716 Langer R, V. J. P. (1993). Tissue Engineering. *Science*, *260*(5110), 920–926.

717 Langer, R. (1997). Tissue Engineering: A New Field and Its Challenges . *Pharmaceutical Research*,
718 *14(7)*(7), 840–841.

719 Lemons, B. D. R. S. H. J. S. E. (Ed.). (2013). SECTION II.6 - Applications of Biomaterials in Functional
720 Tissue Engineering. In *Biomaterials Science (Third Edition)* (pp. 1119–1122). Academic Press.
721 http://doi.org/http://dx.doi.org/10.1016/B978-0-08-087780-8.00108-X

722 Li, M., Mondrinos, M. J., Gandhi, M. R., Ko, F. K., Weiss, A. S., & Lelkes, P. I. (2005). Electrospun
723 protein fibers as matrices for tissue engineering. *Biomaterials*, *26*(30), 5999–6008.
724 http://doi.org/http://dx.doi.org/10.1016/j.biomaterials.2005.03.030

725 Liu, C., Xia, Z., & Czernuszka, J. T. (2007). Design and Development of Three-Dimensional Scaffolds for
726 Tissue Engineering. *Chemical Engineering Research and Design*, *85*(7), 1051–1064.
727 http://doi.org/http://dx.doi.org/10.1205/cherd06196

728 Liu, Y., & Chan-Park, M. B. (2009). Hydrogel based on interpenetrating polymer networks of dextran and
729 gelatin for vascular tissue engineering. *Biomaterials*, *30*(2), 196–207.
730 http://doi.org/http://dx.doi.org/10.1016/j.biomaterials.2008.09.041

731 Lutolf, M. P., & Hubbell, J. A. (2005). Synthetic biomaterials as instructive extracellular
732 microenvironments for morphogenesis in tissue engineering. *Nature Biotechnology*, *23*(1), 47–55.
733 http://doi.org/http://dx.doi.org/10.1038/nbt1055

734 MARRS, W. M. (1982). GELATIN CARBOHYDRATE INTERACTIONS AND THEIR EFFECT ON
735 THE STRUCTURE AND TEXTURE OF CONFECTIONERY GELS. *PROGRESS IN FOOD AND*
736 *NUTRITION SCIENCE*, *6*(1-6), 259–268.

737 Mendes, S. C., Reis, R. ., Bovell, Y. P., Cunha, A. ., van Blitterswijk, C. A., & de Bruijn, J. D. (2001).
738 Biocompatibility testing of novel starch-based materials with potential application in orthopaedic
739 surgery: a preliminary study. *Biomaterials*, *22*(14), 2057–2064. http://doi.org/10.1016/S0142-
740 9612(00)00395-1

741 Nichol, J. W., Koshy, S. T., Bae, H., Hwang, C. M., Yamanlar, S., & Khademhosseini, A. (2010). Cell-
742 laden microengineered gelatin methacrylate hydrogels. *Biomaterials*, *31*(21), 5536–5544.
743 http://doi.org/http://dx.doi.org/10.1016/j.biomaterials.2010.03.064

744 Peng, C.-K., Yu, S.-H., Mi, F.-L., & Shyu, S.-S. (2006). Polysaccharide-based artificial extracellular
745 matrix: Preparation and characterization of three-dimensional, macroporous chitosan and chondroitin
746 sulfate composite scaffolds. *Journal of Applied Polymer Science*, *99*(5), 2091–2100.
747 http://doi.org/10.1002/app.22730

748 Pescosolido, L., Piro, T., Vermonden, T., Coviello, T., Alhaique, F., Hennink, W. E., & Matricardi, P.
749 (2011). Biodegradable IPNs based on oxidized alginate and dextran-HEMA for controlled release of
750 proteins. *Carbohydrate Polymers*, *86*(1), 208–213.
751 http://doi.org/http://dx.doi.org/10.1016/j.carbpol.2011.04.033

752 Peters, K., Salamon, A., Van Vlierberghe, S., Rychly, J., Kreutzer, M., Neumann, H.-G., … Dubruel, P.
753 (2009). A New Approach for Adipose Tissue Regeneration Based on Human Mesenchymal Stem
754 Cells in Contact to Hydrogels—an In Vitro Study. *Advanced Engineering Materials*, *11*(10), B155–
755 B161. http://doi.org/10.1002/adem.200800379

756 Picard, J., Doumèche, B., Panouillé, M., & Larreta-Garde, V. (2010). Gelatin-Polysaccharide Mixed
757 Biogels: Enzyme-Catalyzed Dynamics and IPNs. *Macromolecular Symposia*, *291-292*(1), 337–344.
758 http://doi.org/10.1002/masy.201050540

759 Puppi, D., Chiellini, F., Piras, A. M., & Chiellini, E. (2010). Polymeric materials for bone and cartilage
760 repair. *Progress in Polymer Science*, *35*(4), 403–440.
761 http://doi.org/http://dx.doi.org/10.1016/j.progpolymsci.2010.01.006

762 Raafat, A. I., Eldin, A. A. S., Salama, A. A., & Ali, N. S. (2013). Characterization and bioactivity
763 evaluation of (starch/N-vinylpyrrolidone)hydroxyapatite nanocomposite hydrogels for bone tissue
764 regeneration. *JOURNAL OF APPLIED POLYMER SCIENCE*, *128*(3), 1697–1705.
765 http://doi.org/10.1002/app.38113

766 Ramadhar, T. R., Amador, F., Ditty, M. J. T., & Power, W. P. (2008). Inverse H-C ex situ HRMAS NMR
767 experiments for solid-phase peptide synthesis. *Magnetic Resonance in Chemistry*, *46*(1), 30–35.
768 http://doi.org/10.1002/mrc.2118

769 Rueda, J., Suica, R., Komber, H., & Voit, B. (2003). Synthesis of New Polymethyloxazoline Hydrogels by
770 the "Macroinitiator" Method. *Macromolecular Chemistry and Physics*, *204*(7), 954–960.
771 http://doi.org/10.1002/macp.200390065

Salamon, A., van Vlierberghe, S., van Nieuwenhove, I., Baudisch, F., Graulus, G.-J., Benecke, V., … Peters, K. (2014). Gelatin-Based Hydrogels Promote Chondrogenic Differentiation of Human Adipose Tissue-Derived Mesenchymal Stem Cells In Vitro. *Materials*, *7*(2), 1342–1359. http://doi.org/10.3390/ma7021342

Sandra Van Vlierberghe José C. Martins, and Peter Dubruel, B. F. (2010). Hydrogel Network Formation Revised: High-Resolution Magic Angle Spinning Nuclear Magnetic Resonance as a Powerful Tool for Measuring Absolute Hydrogel Cross-Link Efficiencies. *Applied Spectroscopy*, *64*(10), 1176–1180.

Shapiro, M. J., Chin, J., Marti, R. E., & Jarosinski, M. A. (1997). Enhanced resolution in MAS NMR for combinatorial chemistry. *Tetrahedron Letters*, *38*(8), 1333–1336. http://doi.org/http://dx.doi.org/10.1016/S0040-4039(97)00092-0

Shin, H., Jo, S., & Mikos, A. G. (2003). Biomimetic materials for tissue engineering. *Biomaterials*, *24*(24), 4353–4364. http://doi.org/http://dx.doi.org/10.1016/S0142-9612(03)00339-9

Silver, F. H., Bradica, G., & Tria, A. (2002). Elastic energy storage in human articular cartilage: estimation of the elastic modulus for type II collagen and changes associated with osteoarthritis. *Matrix Biology*, *21*(2), 129–137. http://doi.org/http://dx.doi.org/10.1016/S0945-053X(01)00195-0

Turgeon, S. L., & Beaulieu, M. (2001). Improvement and modification of whey protein gel texture using polysaccharides. *Food Hydrocolloids*, *15*(4–6), 583–591. http://doi.org/http://dx.doi.org/10.1016/S0268-005X(01)00064-9

V, A. J., V, C. A., J, H., M, H., K, H., G, J. R., … T, S. R. F. (2007). Definitions of terms relating to the structure and processing of sols, gels, networks, and inorganic-organic hybrid materials (IUPAC Recommendations 2007). *Pure and Applied Chemistry*. http://doi.org/10.1351/pac200779101801

Van Den Bulcke, A. I., Bogdanov, B., De Rooze, N., Schacht, E. H., Cornelissen, M., & Berghmans, H. (2000). Structural and Rheological Properties of Methacrylamide Modified Gelatin Hydrogels. *Biomacromolecules*, *1*(1), 31–38. http://doi.org/10.1021/bm990017d

Van Nieuwenhove, I., Van Vlierberghe, S., Salamon, A., Peters, K., Thienpont, H., & Dubruel, P. (2015). Photo-crosslinkable biopolymers targeting stem cell adhesion and proliferation: the case study of gelatin and starch-based IPNs. *Journal of Materials Science: Materials in Medicine*, *26*(2), 104. http://doi.org/10.1007/s10856-015-5424-4

Wang, H., Zhou, L., Liao, J., Tan, Y., Ouyang, K., Ning, C., … Tan, G. (2014). Cell-laden photocrosslinked GelMA-DexMA copolymer hydrogels with tunable mechanical properties for tissue engineering. *JOURNAL OF MATERIALS SCIENCE-MATERIALS IN MEDICINE*, *25*(9), 2173–2183. http://doi.org/10.1007/s10856-014-5261-x

Whitehouse, A. S., Ashby, P., Abeysekera, R., & Robards, A. W. (1996). Phase behaviour of biopolymers at high solid concentrations. In Phillips, GO and Williams, PA and Wedlock, DJ (Ed.), *GUMS AND STABILISERS FOR THE FOOD INDUSTRY 8* (pp. 287–295). OXFORD UNIVERSITY PRESS GREAT CLAREDON ST, OXFORD OX2 6DP, ENGLAND: IRL PRESS.